Electronic Supplementary Material (ESI) for CrystEngComm.

SUPPORTING INFORMATION

Supplementary Material

Humidity-responsive Self-Assembly of Short Peptides with Super-flexibility

Zhongjie Zhu[a,b], Jinrong Yang[c,*], Hongwei Zhao[a,b,*], Yu Wu[b], Tanglong Bai[d], Hongti Zhang[d], Yongshun Song[e], Te Ji[a], Jun Hu[a,b], Yi Gao[a,*]

[a] Shanghai Advanced Research Institute, Chinese Academy of Sciences, Shanghai, 201210, China
[b] Shanghai Institute of Applied Physics, Chinese Academy of Sciences, Shanghai, 201800, China
[c] School of Chemistry and Molecular Engineering, East China Normal University, Shanghai, 200062, China
[d] School of Physical Science and Technology, ShanghaiTech University, Shanghai, 201210, China
[e] East China University of Science and Technology, Shanghai, 200237, China

1. Experimental and Methods

1.1 Materials and sample preparation

The Gly (≥98%, G), GlyGly (≥99%, *ext*-GG), GlyGlyGly (≥99%, *ext*-GGG) were purchased from J&K. The aqueous solutions were prepared with 18.2 MΩ, 3 ppb TOC Milli-Q water (Millipore, US). The milled raw materials powders were placed in a water vapor container with high humidity at room temperature. The *ext*-GG and *ext*-GGG were added in pure water repeatedly with shaking to achieve dissolution equilibrium, the *ext*-GGG concentrations were 73 mg/mL at room temperature (25 °C), which were stored at 2 °C.

1.2 Powder X-ray diffraction (PXRD)

The PXRD patterns of samples were measured using a Bruker D8 Advance (Cu source, 40 kV voltage, 40 mA filament emission). The data were collected within a scan range of 5° to 90° (2θ), the scanning rate was 0.2° s^{-1}.

1.3 Single Crystal X-ray Diffraction (SCXRD)

SCXRD data was collected on a Bruker D8-Venture single-crystal X-ray diffractometer equipped with a Turbo X-ray source (Mo Kα radiation, $\lambda = 0.71073$ Å) adopting the direct-drive rotating-anode technique and a CMOS detector. The data frames were collected using the APEX3 program and processed using the SAINT routine. The empirical absorption correction was applied using the SADABS program. The structure was solved by Intrinsic Phasing with ShelXT and refined with ShelXL using OLEX2 [1].

Micro-crystals formed in glass tubes were subjected to the beamline National Facility for Protein Science Shanghai (NFPS) -BL17B at Shanghai Synchrotron Radiation Facility (SSRF). The collection of SCXRD data at 100 K using the wavelength of 0.65251 Å and Dectris Pilatus3-2M detector.

1.4 Scanning electron microscopy (SEM)

On a LEO 1530VP, the samples were mounted on carbon tape and analyzed using 7 kV with a working distance of 6.2 mm. The images used in this work were magnified at 5000×. No further image processing was performed.

1.5 Thermogravimetry and differential scanning calorimetry (TG-DSC)

TG-DSC was performed using on STA 449 F3 Jupiter (NETZSCH). Sample was put in a graphite crucible with lip on it (GGGH: 3.21 mg), and heated ranging from 32 to 398 °C with a heating rate of 10 K/min under Ar atmosphere (60 mL/min). The software used for the data evaluation was Origin.

1.6 *In situ* nanomechanical characterizations

The basic setup of the *in situ* tensile test platform for individual single crystal GGGH microfibers was based on a push-to-pull micromechanical device (MMD) actuated by a quantitative picoindenter (Hysitron PI 88 PicoIndenter). To prevent possible damages to sample's structure and morphology, we applied conductive silver epoxy glue (Chemtronics, CircuitWorks Conductive Epoxy) to clamp the individual single crystal onto the sample stages of the MMD. The picoindenter was used inside a field-emission scanning electron microscope (SEM, JEOL JSM-IT500HR), and the corresponding deformation process of the tested samples was directly monitored and recorded by the SEM. The tensile tests were performed under displacement control mode with constant strain rates of ~ 0.0011 s^{-1}.

1.7 Methods of calculations

The B3LYP method together with 6-311G (d, p) basis sets were used to optimize the molecular geometries of two GGG without water molecule and with four water molecules for all stationary points. The corresponding harmonic vibrational frequencies were performed to determine the nature of the stationary points and to provide the thermodynamic contributions to the free energy. These calculations were all carried out with the Gaussian 09 program package [2]. For the entropy calculation of the configuration of GGG in *ext*-GGG, PPII, Turn, GGGH, 3_{10}-helix and α-helix, we constrained the backbone of these configurations within the optimization process and preform frequency calculation to obtain the entropy information.

Information about electronic supplementary material.

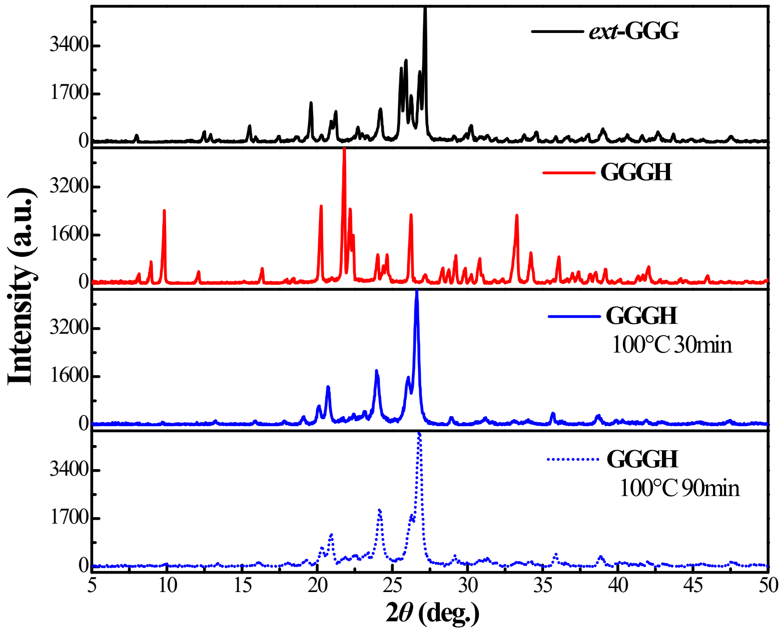

Figure S1. XRD spectra of ext-GGG, GGGH and samples heated at 100 ℃.

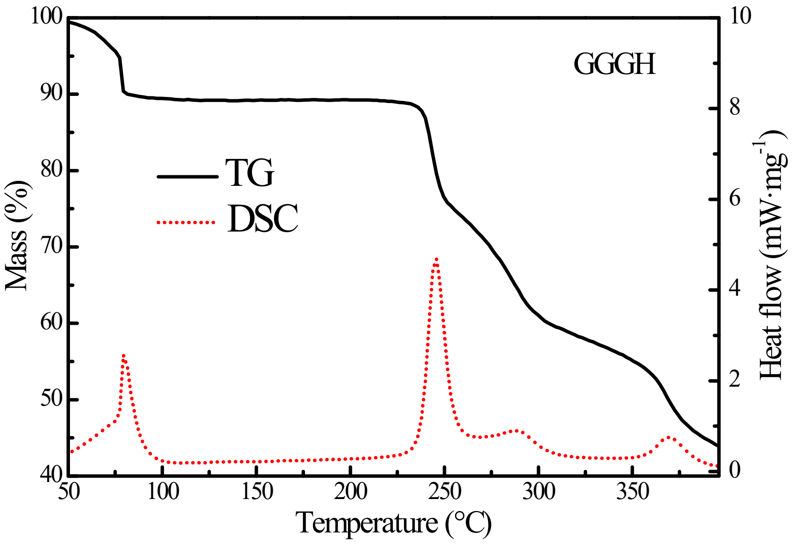

Figure S2. The TG-DSC curves during the thermal decomposition of GGGH at different mass at the heating rate of 10 K/min in Ar.

we further followed up the stability of the sample. The experimental results show that GGGH powders remained unchanged for several months at room temperature with exceptional stability. Figure S1 shows the comparison between the raw material and the recrystallized hydrate GGGH and its heating. The results show that when the hydrate is heated at 100 ℃ for 30 min, its diffraction peak has similar characteristics to that of the raw material. The diffraction peak near 10° disappears, and the intensity of the diffraction peak near 20°, 22°, and 33° decreases significantly. The intensity of the diffraction peak near 26° increases significantly. When the heating time increased to 90 min, the diffraction peak did not change. It indicates that the temperature becomes stable after heating for 30 minutes. At the same time, the TG-DSC curve of GGGH under dynamic conditions is disclosed in Figure S2. The figure shows that there are two complicated pyrolysis processes within the tested temperature range, which predicts that the kinetic analysis of GGGH can be complicated to describe a multiple reaction process. The above results indicate that the sample exhibits good thermal stability in the temperature range of 32 to 60 ℃. It is unstable in the temperature range of 60 to 100 ℃ and has a first obvious weight loss phenomenon, which is preliminarily proved to be a dehydration reaction. It is clearly seen in Figure S1 that the thermal decomposition process only consists of an exothermic stage, indicating that it has undergone decomposition. It is further demonstrated that water molecules play an important role in the formation of GGGH structure. Therefore, our next step was to conduct a detailed test of the effect of water molecules on *ext*-GGG.

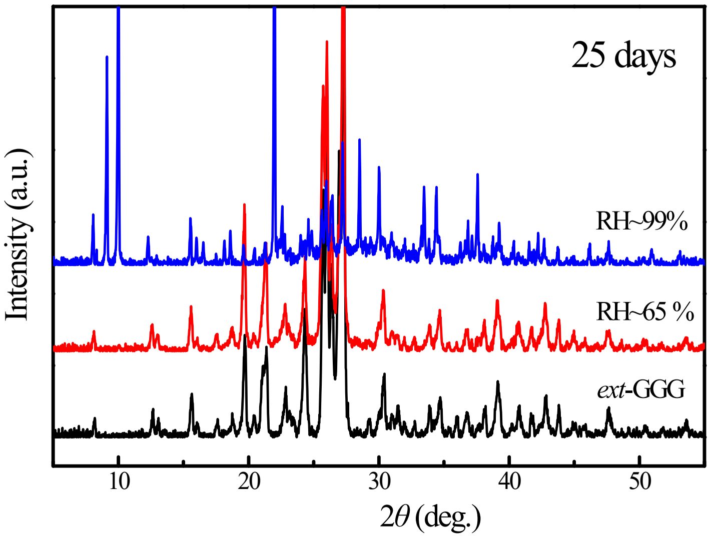

Figure S3. The PXRD patterns of *ext*-GGG raw materials at different humidity.

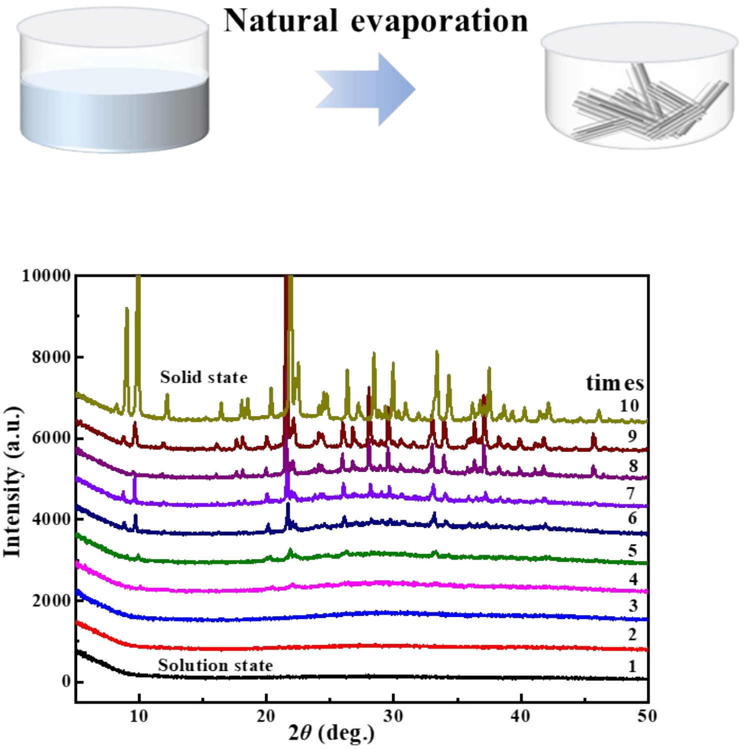

Figure S4. PXRD Schematics of ext-GGG in Solid State after Transition from Solution.

we also compared the diffraction peak changes of *ext*-GGG samples at different humidity levels over the same duration (see Figure S3). And we placed *ext*-GGG near-saturated solution on a substrate with grooves and allowed the solution to naturally evaporate at room temperature over a short period. Simultaneously, we continuously monitored the diffraction signals of the samples through XRD testing, as shown in Figure S4. The experiment revealed that with the reduction in solvent, new diffraction peaks appeared by the fifth test, and with increasing test repetitions, diffraction peaks of all GGGH crystals were observed, consistent with the hydrated crystal form of triglyceride (GGG) adopts proline II (PPII) conformation reported by Guo et al.[3] . Furthermore, these experiments further underscore the significance of humidity as a critical factor in sample transformations.

Table S1. Detailed parameter information of several helix structures.

Types of helical	Pitch	Rise per residue	H-bond	Dihedral angle ϕ, ψ
PPII helix	9.3 Å	3.0 Å	No	(ϕ, ψ): (-75°, +145°)
GGG-helix	4.7 Å	0.78 Å	*i*, *i*+5	(ϕ, ψ): (±81°, ∓136°)
α-helix	5.4 Å	1.5 Å	*i*, *i*+4	(ϕ, ψ): (±57°, ±47°)
π-helix	4.8 Å	1.1 Å	*i*, *i*+5	(ϕ, ψ): (-57°, -70°)
3_{10}-helix	6.0 Å	2.0 Å	*i*, *i*+3	(ϕ, ψ): (-74°, -4°)

(The data of PPII helix, α-helix, π-helix, 3_{10} helix from ref.[4,5].)

SI References

[1] O.V. Dolomanov, Bourhis, L. J., Gildea, R. J., Howard, J. A. K., Puschmann, H., OLEX2: a complete structure solution, refinement and analysis program, J. Appl. Crystallogr. 42 (2009) 339-341.
[2] M.J. Frisch, Trucks, G. W., Schlegel, H. B., Scuseria, G. E., Robb, M. A., Cheeseman, J. R., Scalmani, G., Barone, V., Mennucci, B., Petersson, G. A., Gaussian 09, Revision A.1, Inc., Wallingford CT (2009).
[3] M. Guo, I. Rosbottom, L. Zhou, C. Yong, L. Zhou, Q. Yin, I. Todorov, E. Errington, J. Heng, Triglycine (GGG) Adopts a Polyproline II (pPII) Conformation in Its Hydrated Crystal Form: Revealing the Role of Water in Peptide Crystallization, J. Phy. Chem. Lett. 12 (2021) 8416-8422. 10.1021/acs.jpclett.1c01622.
[4] J.C. Horng, Raines, R. T., Stereoelectronic effects on polyproline conformation, Protein Sci 15 (2006) 74-83.
[5] S. Choudhuri, Additional Bioinformatic Analyses Involving Protein Sequences, Elsevier Inc.2014.